

# Temporal Controls on Basalt Genesis and Evolution on the Owyhee Plateau, Idaho and Oregon

Kurt A. Shoemaker<sup>1</sup> and William K. Hart<sup>2</sup>

## ABSTRACT

The development of the Snake River Plain volcanic province has been attributed to the passage of the North American plate over the Yellowstone mantle plume. As this province was being formed by an eastward progression of younger silicic volcanic centers, basaltic volcanism has continued through the present day in the western regions of the "plume track." Of particular interest is the Owyhee Plateau of southeastern Oregon, located at the westernmost end of the SRP volcanic province. The Owyhee Plateau preserves the best documented continuous record of mid-Miocene to Recent basaltic volcanism in the northwestern United States, allowing an investigation of variations in magmatic sources and processes through time. In addition, this region is underlain by lithosphere transitional between that of the Proterozoic-Archean Wyoming Craton to the east and accreted terranes younger than 200 Ma to the west. Basaltic products that erupted from a variety of vents on the Owyhee Plateau illustrate chemical and Sr isotopic diversity that cannot be solely attributed to lateral lithospheric heterogeneities. Rather, this diversity appears to be a function of eruptive age. For example, Sr isotope data show a systematic increase in  $^{87}\text{Sr}/^{86}\text{Sr}$  from 0.704 to 0.707 with decreasing age from 17.5-11 Ma, but decreasing  $^{87}\text{Sr}/^{86}\text{Sr}$  to 0.704 from 11-0 Ma. The "peak" in Sr values corresponds to a regional change in the dominant basalt type erupted, from large volume, strongly fractionated basalts and basaltic andesites before 11 Ma to smaller volume,

more primitive high-alumina olivine tholeiites after 11 Ma. A preliminary model is offered that calls for temporal variations in magma production, lithospheric structure, and the relative contributions from lithospheric and sublithospheric source reservoirs.

Key words: basalt, Owyhee Plateau, lithosphere, Sr isotopes, magmatic evolution, plume track

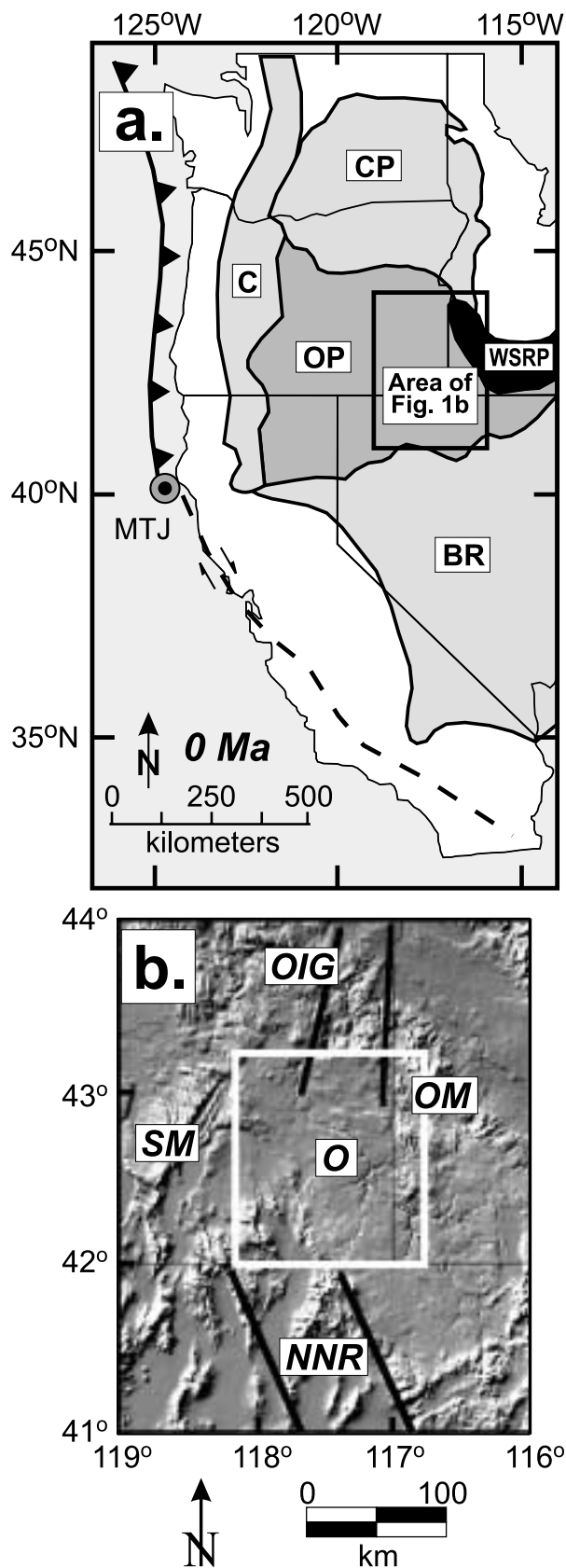
## INTRODUCTION

The initiation of flood basalt volcanism in the northwestern United States at approximately 17.5 Ma marks the onset of a time and longitudinally transgressive sequence of volcanic activity attributed to the passage of the North American plate over the hypothesized Yellowstone mantle plume (Pierce and Morgan, 1992; Geist and Richards, 1993; Camp, 1995). The earliest pulse of flood basalt eruptions (17.5-14 Ma) are represented by the Clarkston Basalt of the Columbia Plateau (Hooper and Hawkesworth, 1993) and Steens Mountain Basalt of the Oregon Plateau (Carlson and Hart, 1987, 1988; Hart and Carlson, 1987). These basalts were erupted from a narrow array of vents extending for nearly 1,000 km from southeastern Washington to central Nevada. This array is believed to represent a rift in the back-arc region of the Cascade arc (Christiansen and McKee, 1978; Carlson and Hart, 1987; Zoback and others, 1994). After 14 Ma, eruptive activity along this rift contracted in a north-south direction, becoming focused in the Owyhee Plateau of the Oregon-Idaho-Nevada border region (Figure 1). Subsequent magmatism to the east formed the Snake River Plain (SRP). It is important to note that, as the SRP was being formed by an eastward progression of silicic eruptive centers, basaltic volcanism has continued essentially

*Editors' note: The manuscript was submitted in June 1998 and has been revised at the authors' discretion.*

<sup>1</sup>Geology Department, Saint Joseph's College, Rensselaer, IN 47978

<sup>2</sup>Geology Department, Miami University, Oxford OH 45056



through the present day in the western regions of the “plume track.”

Determining the ultimate mantle sources of and the processes responsible for the evolution of these basalts has been hindered by the complication of contamination of the primary magmas by chronologically and chemically heterogeneous lithospheric materials (Leeman and others, 1992). Regional geochemical and isotopic information, combined with regional patterns of crustal deformation, has led some researchers to argue that the initial, large volume flood basalt eruptions were related to the arrival of the Yellowstone plume head at the base of the lithosphere (Geist and Richards, 1993; Hooper and Hawkesworth, 1993; Camp, 1995). Other researchers have used the same evidence to argue that these basalts were erupted as a result of rifting behind the Cascade volcanic arc (Christiansen and McKee, 1978; Carlson and Hart, 1987). Obviously, the current data base is ambiguous with regard to these issues, and questions concerning sources and processes cannot be answered until the influence of the lithosphere on the primary magmas can be adequately determined (Hart, 1997; Hart and others, 1997).

The Owyhee Plateau (Figure 1) provides an excellent opportunity to explore variations in the geochemical and isotopic characteristics of late Cenozoic northwestern United States basalts through time. The basalts in this study constitute a geochemically and isotopically diverse suite erupted over the past 17.5 Ma from vents located within a geographically restricted area between approximately lat 42°00'N. and 43°15'N. and long 116°45'W. and 118°15'W. This area is underlain by lithosphere transitional between that of the Proterozoic-Archean Wyoming craton to the east and accreted terranes younger than 200 Ma to the west (Leeman and others, 1992). Here, the basaltic magmas are assumed to have passed through, and consequently to have had the opportunity to interact with, the same chronologically similar “package” of lithospheric materials. Thus, by eliminating the distinct isotopic signatures attributed to regional, lateral lithospheric variations, a significant variable to investigate is time.

Figure 1. Location of the study area, in relation to major volcanic and tectonic features of the western United States. (a) Generalized map of the major late Cenozoic volcanic provinces of the northwestern United States. C: Cascade arc; CP: Columbia Plateau; OP: Oregon Plateau; WSRP: Western Snake River Plain; BR: Basin and Range; MTJ: Mendocino Triple Junction. (b) Digital elevation model of the Owyhee Plateau study area, modified from Sterner (1997). SM: Steens Mountain; OM: Owyhee Mountains; OIG: Oregon-Idaho Graben; NNR: Northern Nevada Rift; O: Owyhee Plateau and Owyhee River Canyon region. Locations of tectonic and structural features adapted from Bohannon and Parsons (1995), Zoback and others (1994), Carlson and Hart (1987), and Ferns (1997).

Furthermore, to our knowledge, the Owyhee Plateau contains the most complete record of mid-Miocene to Recent basaltic volcanism in the northwestern United States. Thus, it is uniquely suited to an exploration of the temporal variations in lithospheric and sublithospheric contributions to this late Cenozoic basaltic volcanism.

### SPATIAL AND TEMPORAL RELATIONSHIPS

Previous investigations of post-17.5 Ma Oregon Plateau basaltic volcanism by Carlson and Hart (1987, 1988), Hart and Carlson (1987, 1992), and Draper (1991) documented a significant change about 11 Ma in the dominant basalt type erupted (Figure 2a). The older eruptions (Steens Mountain Basalt) produced strongly fractionated tholeiitic basalts and basaltic andesites. Post-11 Ma eruptions were dominated by less fractionated low-K, high alumina olivine tholeiites (HAOT). This change coincides not only with the regional shift from large volume, fissure-fed eruptions to small volume eruptions from discrete eruptive centers, but also with the onset of regional lithospheric thinning due to diffuse extension throughout the entire Oregon Plateau area (Hart and Carlson, 1987; Hooper, 1990; Draper, 1991).

Leeman and others (1992) documented that the maximum diversity in  $^{87}\text{Sr}/^{86}\text{Sr}$  for late Cenozoic northwestern United States basalts occurs in a longitudinal “band” corresponding to approximately  $117^\circ$  to  $118^\circ$  west longitude (Figure 2b). This region of maximum diversity coincides with the transition between the Proterozoic-Archean cratonic lithosphere to the east and accreted terranes younger than 200 Ma to the west (Leeman and others, 1992; Elison and others, 1990; Wright and Wooden, 1991). Importantly, the Owyhee Plateau overlies this region of transitional lithosphere (Figure 1).

Hart (1997) further explored the relationships between age and location of eruption and Sr isotope compositions of northwestern United States basalts (Figure 3). Figure 3 substantiates the observations of Leeman and others (1992) that a wide range in basalt  $^{87}\text{Sr}/^{86}\text{Sr}$  values occurs along approximately  $117^\circ$  west longitude, with higher and lower  $^{87}\text{Sr}/^{86}\text{Sr}$  values occurring east and west of this line, respectively. Additionally, Figure 3 shows that those basalts representing the earliest pulse of volcanism (Steens, Clarkston, and Picture Gorge basalts) have lower  $^{87}\text{Sr}/^{86}\text{Sr}$  values than many of the samples representing younger eruptions (e.g., SRP and Saddle Mountains basalts). Furthermore, samples from the Owyhee Plateau define a wide range in  $^{87}\text{Sr}/^{86}\text{Sr}$ , from less than 0.704 to greater than 0.707. Another interesting relationship is

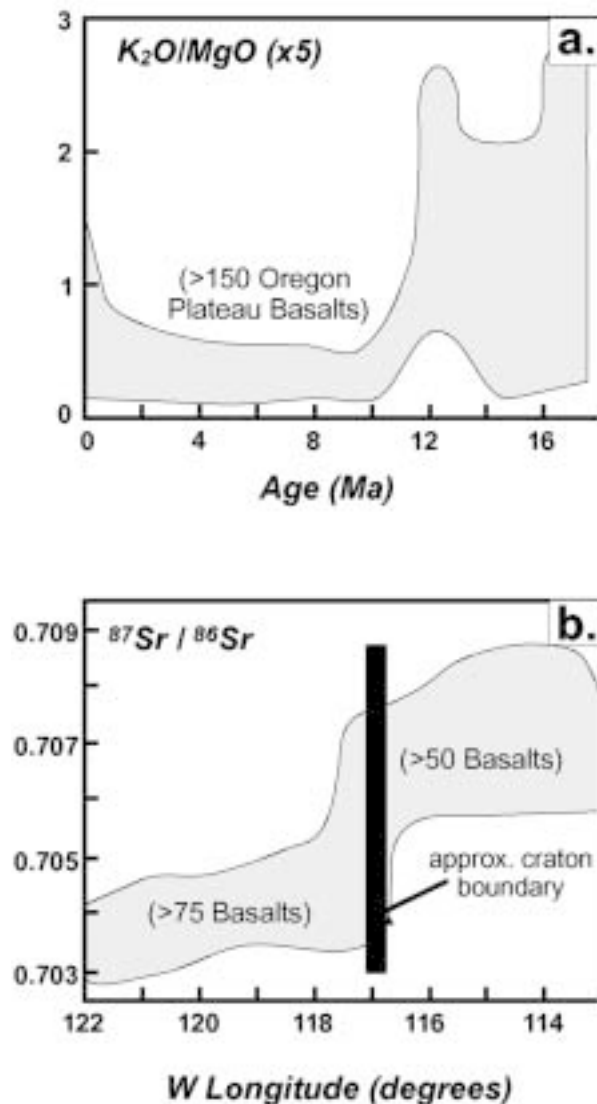


Figure 2. Important regional geochemical and isotopic observations. (a) Illustration of the regional change in basalt geochemistry on the Oregon Plateau, from strongly fractionated basalts and basaltic andesites before approximately 11 Ma to relatively unfractionated basalts after approximately 11 Ma, after Hart and Carlson (1987). (b) Longitudinal variation in Sr isotope compositions of basaltic rocks, after Leeman and others (1992). The area of focus for this study coincides with the cratonic boundary, where the greatest diversity in  $^{87}\text{Sr}/^{86}\text{Sr}$  is observed.

found when the data are plotted versus the age of eruption. Sr-isotope values increase with decreasing age from the initiation of volcanism to about 11 Ma, at which point the data diverge. Except for the young Yellowstone area basalts that span nearly the entire observed range in  $^{87}\text{Sr}/^{86}\text{Sr}$ , SRP basalts retain radiogenic signatures while Owyhee Plateau basalts trend toward lower  $^{87}\text{Sr}/^{86}\text{Sr}$  values from 11 Ma to 0 Ma. The rest of this paper will focus only on the Owyhee Plateau basalts.

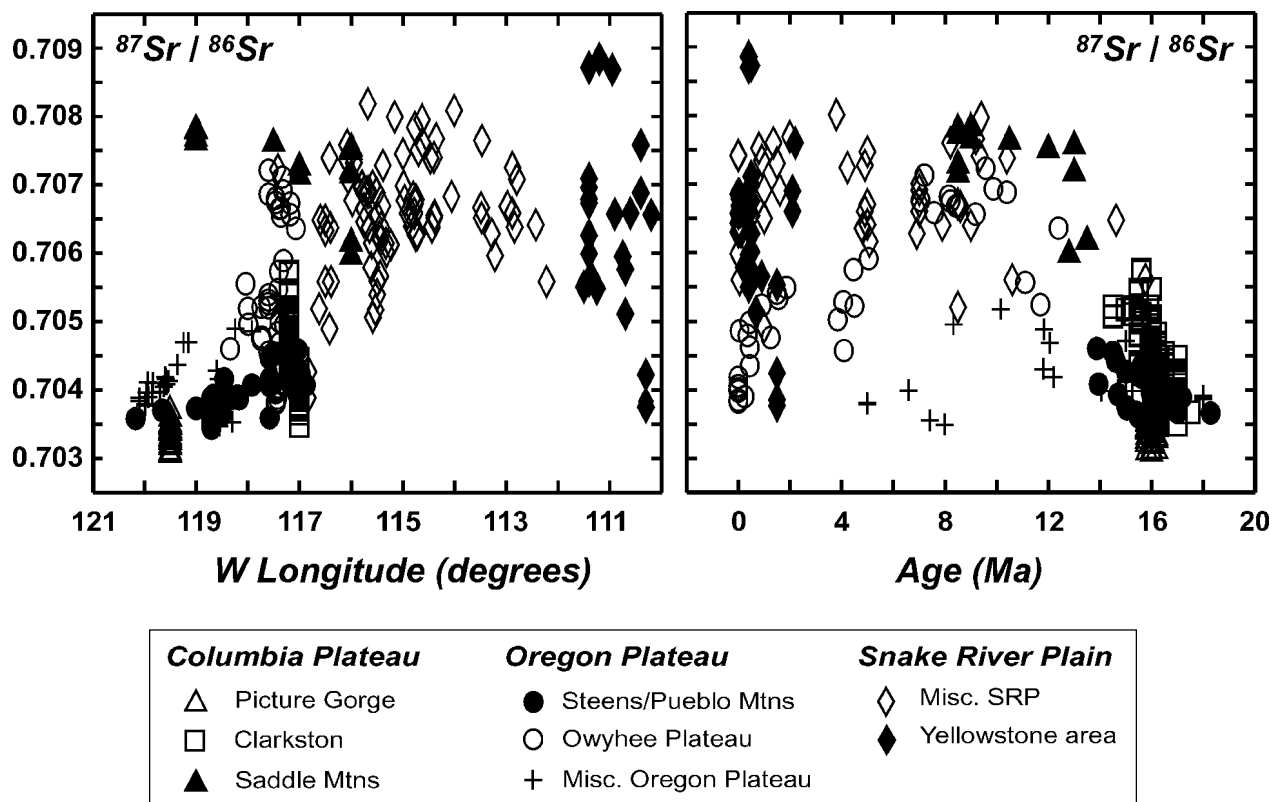


Figure 3. Compilation of Sr isotope data for northwestern United States basalts, after Hart (1997). Where possible, the longitude of the eruption site is used. Data are from Carlson (1984), Carlson and Hart (1987), Carlson and others (1981), Hart (1985), Hart and others (1989), Hooper and Hawkesworth (1993), Lambert and others (1995), Leeman and others (1992), Leeman (1982), Leeman and Manton (1971), Mark and others (1975), Noble and others (1973), and this study.

## DATA

### CHRONOSTRATIGRAPHY

Careful sampling of basalt flow sequences exposed in fault scarps and in canyons of the Owyhee River and its tributaries (see Figure 1b) combined with new (Table 1) and previously reported (Hart and Mertzman, 1982, 1983; Hart and Carlson, 1983, 1985; and Hart and others, 1984) chronologic data has allowed us to construct a composite chronostratigraphic section representing the history of basaltic volcanism on the Owyhee Plateau over the last 17.5 Ma. Four new  $^{40}\text{Ar}/^{39}\text{Ar}$  method age determinations (Table 1) were obtained in order to better constrain the timing of the older pulse of Owyhee Plateau basaltic volcanism. Age estimates were interpolated for samples with relatively tight (approximately 2 m.y. or less) stratigraphic constraints based on K-Ar or  $^{40}\text{Ar}/^{39}\text{Ar}$  age data. These estimated ages are marked with an asterisk (\*) in Table 2.

On the basis of eruptive age, the sample suite has been divided into five groups as indicated in Figure 4. These groups are described briefly below:

**17.5-14 Ma.** This interval represents the initial, large volume eruptive phase of Oregon Plateau basaltic volcanism, temporally correlative with the eruption of the Clarkston Basalt of the Columbia Plateau (Hart and Carlson, 1985; Hart and others, 1989; Hooper and Hawkesworth, 1993). These flood basalts typically were erupted from isolated fissures and large fissure systems. Magmas erupted at this time were strongly fractionated basalts to basaltic andesites with tholeiitic to calc-alkaline affinities.

**14-11 Ma.** This interval represents the waning stages of Steens Mountain Basalt eruptions. Basalt compositions are similar to those of the older age group, but the volumes erupted are significantly smaller and individual flows are less areally extensive (Hart and Mertzman, 1982; Hart and Carlson, 1985).

**11-6 Ma.** This interval marks the regional change in dominant basalt type erupted, from the strongly fraction-

Table 1. New  $^{40}\text{Ar}/^{39}\text{Ar}$  age data.

Sample number	Age Analysis	steps	$^{39}\text{ArK}$ ( $\times 10^{-15}$ mol)	% $^{39}\text{Ar}$	K/Ca	Age (Ma)	$\pm 2$ s.d. (Ma)
H85-10A	plateau	6	46.6	82.2	0.33	16.27	0.17
JV96-2	plateau	5	33.4	75.2	0.09	12.37	0.48
JV96-4	plateau	7	27.8	73.1	0.20	14.61	0.35
JV96-7	plateau	7	90.1	66.0	0.28	13.87	0.39

Correction factors:

$$(^{39}\text{Ar}/^{37}\text{Ar})\text{Ca} = 0.00070 \pm 0.00005$$

$$(^{36}\text{Ar}/^{37}\text{Ar})\text{Ca} = 0.00026 \pm 0.00002$$

$$(^{38}\text{Ar}/^{39}\text{Ar})\text{K} = 0.0119$$

$$(^{40}\text{Ar}/^{39}\text{Ar})\text{K} = 0.0002 \pm 0.0003$$

ated basalts and basaltic andesites of the early phase of volcanism to relatively unfractionated basalts. This is accompanied by a change from primarily fissural flood basalt activity to a combination of eruptions from local fissures associated with extensional features and from isolated low shield cones similar to those found within the SRP proper. Compositions range from low-K, low-Ti, high alumina olivine tholeiites (HAOT) to high-K, high-Ti Snake River Plain-type olivine tholeiites (SROT). A full spectrum of compositions transitional between these end members (transitional basalts, TB) is present (Hart and others, 1984; Hart, 1985).

*6-3 Ma.* This interval is defined primarily by increased magmatism between 5-4 Ma following a brief period of low magmatic output (Hart and others, 1984; Figure 3). Magmatism during this interval is dominated by small volume HAOT to SROT eruptions from local fissures and low shield cones (Hart and others, 1984; Hart, 1985).

*3-0 Ma.* This interval again follows a brief period of low magmatic output and is dominated by small volume HAOT eruptions (Hart and others, 1984). In addition, the only alkaline basalts observed on the Oregon Plateau were produced during this interval (after 1 Ma) and were erupted from low shield and tephra cones (Hart and Mertzman, 1983; Russell and others, 1988; Hart, 1996).

## ELEMENTAL AND SR-ISOTOPE GEOCHEMISTRY

Major and trace element geochemical, Sr-isotope, and chronologic data for the sample suite of this study are given in Table 2. Major element analyses were performed by both X-ray fluorescence and direct current argon plasma spectrometry (DCP) methods. Samples for which both  $\text{Fe}_2\text{O}_3$  and FeO are reported were analyzed for major elements by XRF at Franklin and Marshall College according to the methods described by Boyd and Mertzman (1987); FeO for these samples was determined

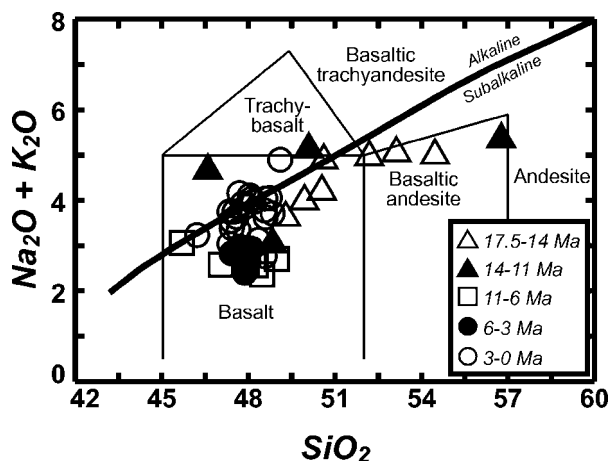


Figure 4. Total alkali-silica diagram of Le Bas and others (1986), showing classification of Owyhee Plateau basalts. Total Fe has been partitioned prior to normalization of analyses to 100 percent anhydrous, according to the method of Le Maitre (1976). Age groups are described in the text.

by titration. Samples for which only  $\text{Fe}_2\text{O}_3$  is reported were analyzed for major elements by DCP at Miami University by the method of external standards, using 7-8 international standards to define calibration curves. All trace elements were analyzed by XRF, with the exception of Sc, V, and Cr, which were determined by DCP using external standards. Sr isotope ratios were determined by thermal ionization mass spectrometry at Miami University and at the Department of Terrestrial Magnetism, Carnegie Institution of Washington. Geochronology by the  $^{40}\text{Ar}/^{39}\text{Ar}$  method was performed at the New Mexico Geochronologic Research Laboratory.

Most of the samples are basalts, although some pre-11 Ma samples plot in the basaltic andesite field of Le Bas and others (1986; Figure 4). The samples are dominantly subalkaline, with the exception of some of the samples representing the most recent pulse of eruptive

Table 2. Major and trace element geochemical, Sr-isotope, and chronologic data for Owyhee Plateau basalts. Major element concentrations are reported as weight percent oxides; trace elements are reported in ppm. Samples are arranged according to eruptive age, from oldest to youngest. Estimated ages are marked with an asterisk (see text). With the exception of estimated ages and ages reported in Table 1, all ages are previously published K-Ar ages (Hart and Mertzman, 1982, 1983; Hart and Carlson, 1983, 1985). Sr isotope data are from Hart (1985), Carlson and Hart (1987), and this study. All Sr isotope ratios are age-corrected initial ratios reported relative to  $^{87}\text{Sr}/^{86}\text{Sr} = 0.70800$  for the E&A  $\text{SrCO}_3$  standard; 2-sigma uncertainties are  $\pm 0.00006$  or less.

	Samples:															
	H85-10A	CH82-32	H85-6	H85-10B	H85-12B	H9-47	JV96-4	JV96-7	JV96-2	H8-74	H9-32	H8-29	H9-37C	SM75-12A	H8-69G	H8-34
Major oxides in wt. %																
SiO <sub>2</sub>	53.82	48.46	49.95	48.72	49.26	49.41	51.89	55.38	48.00	46.13	49.80	49.11	45.48	47.65	48.34	48.42
TiO <sub>2</sub>	2.00	2.20	1.97	2.07	2.54	2.32	1.21	1.04	2.53	2.86	3.00	1.57	2.80	1.25	1.94	1.82
Al <sub>2</sub> O <sub>3</sub>	14.72	15.88	14.73	15.76	16.45	15.18	16.71	16.19	14.20	14.80	15.40	15.89	16.25	16.26	15.53	15.78
Fe <sub>2</sub> O <sub>3</sub>	3.45	12.19	2.93	7.61	9.83	4.85	9.58	8.00	14.05	15.47	7.59	4.77	5.58	2.74	3.36	4.09
FeO	7.09	—	10.41	5.33	3.02	7.56	—	—	—	—	6.40	6.64	8.48	7.33	9.28	7.80
MnO	0.15	0.16	0.25	0.18	0.14	0.19	0.17	0.15	0.20	0.20	0.23	0.19	0.20	0.17	0.20	0.19
MgO	5.01	5.72	2.78	5.67	2.77	4.69	4.88	4.36	6.62	5.01	3.51	7.57	7.50	9.89	8.93	7.35
CaO	7.08	8.17	7.28	9.98	8.66	9.05	8.23	7.09	10.24	8.75	7.24	11.67	9.77	11.49	10.24	11.82
Na <sub>2</sub> O	3.52	3.00	3.15	3.09	3.69	3.19	3.57	3.36	2.51	3.25	3.50	2.38	2.53	2.28	2.23	2.06
K <sub>2</sub> O	1.41	0.93	1.60	0.48	1.06	0.92	1.36	1.86	0.48	1.02	1.60	0.34	0.53	0.34	0.42	0.31
P <sub>2</sub> O <sub>5</sub>	0.47	0.41	0.43	0.26	0.42	0.43	0.67	0.62	0.44	0.98	1.37	0.21	0.50	0.15	0.28	0.27
L.O.I.	1.33	3.16	4.75	1.49	2.61	2.37	0.80	1.37	0.11	0.08	0.73	0.93	0.88	0.72	1.03	1.05
TOTAL	100.05	100.28	100.23	100.64	100.45	100.16	99.06	99.42	99.37	98.55	100.37	101.27	100.50	100.27	101.78	100.96
Trace elements in ppm																
Rb	28	20	44	6.9	17	15	15	40	6.2	16	23	7.4	8.9	6.5	7.5	5.8
Sr	455	440	482	459	561	466	678	595	307	424	468	235	252	201	260	222
Y	36	32	34	29	38	36	31	28	40	48	64	32	36	24	35	35
Zr	263	189	206	146	216	218	206	213	153	270	350	115	159	77	123	156
Nb	11.9	13.8	13.2	9.5	14.9	15.0	14.7	14.5	10.8	23.2	30.5	9.7	14.0	5.6	9.5	10.5
Ni	94	95	63	93	62	49	58	47	86	59	19	118	94	166	145	98
Ga	21.6	22.5	22.0	22.4	24.3	23.1	19.4	18.8	20.7	22.2	22.8	18.5	19.6	16.5	18.3	18.0
Cu	76	74	55	59	72	52	55	45	79	46	31	78	57	89	63	69
Zn	113	124	119	105	116	132	111	103	133	138	167	96	119	77	105	102
U	0.8	1.4	0.3	0.3	0.9	1.7	0.6	1.4	0.1	0.6	1.4	0.7	—	—	—	—
Th	2.6	3.0	5.3	0.6	2.5	4.9	1.8	5.4	—	2.4	1.2	0.6	0.9	1.6	—	0.1
Ba	791	416	662	247	578	538	782	776	548	842	1337	773	574	220	769	352
Ce	45	43	53	40	48	48	74	73	43	65	90	26	43	26	23	27
Co	31	42	35	46	32	39	30	26	45	41	30	46	53	42	52	48
La	23	23	25	16	26	27	34	37	18	38	61	12	24	10	13	15
Cr	177	50	49	33	—	52	114	80	221	70	—	275	53	360	320	288
V	209	280	238	307	—	273	204	158	305	393	—	285	290	240	286	291
Sc	19.5	25.2	21.8	26.9	—	26.0	24.5	19.2	36.6	29.9	—	37.4	32.0	34.7	36.6	37.6
$^{87}\text{Sr}/^{86}\text{Sr}$	0.70432	0.70409	0.70418	0.70397	0.70436	0.70426	0.70442	—	0.70638	0.70521	0.70557	0.70693	0.70723	0.70667	0.70668	0.70675
Age (Ma)	16.27	16.23	*16	*16	*16	15.01	14.61	13.87	12.37	11.70	11.20	9.87	9.57	8.51	8.42	8.21
Latitude	42.73	43.23	42.84	42.73	42.84	42.92	43.21	43.12	42.99	42.92	42.92	42.85	42.79	42.92	42.68	42.55
Longitude	117.05	116.88	117.22	117.05	117.15	116.98	117.14	117.03	117.07	118.00	118.04	117.32	117.60	117.38	117.36	117.18

Table 2. Continued.

Samples:																
	H8-36	H9-39	H9-27	H8-45	H8-47	H9-44	H9-49	H8-50E	H9-37D	H9-36C	H9-36A	H8-75A	H9-42	H9-29	H8-70	H8-57
Major oxides in wt. %																
SiO <sub>2</sub>	47.55	46.34	47.71	47.48	47.79	46.96	46.97	47.87	46.07	47.48	47.42	48.68	46.77	47.08	48.79	48.47
TiO <sub>2</sub>	1.75	2.15	0.81	1.20	1.30	1.57	1.92	1.58	1.88	1.25	0.94	0.88	1.30	1.80	1.94	2.11
Al <sub>2</sub> O <sub>3</sub>	15.07	14.84	16.54	16.82	15.75	16.26	15.89	16.13	15.98	16.03	16.52	16.43	16.58	16.16	16.75	16.35
Fe <sub>2</sub> O <sub>3</sub>	2.25	2.81	1.63	8.34	2.52	3.98	4.81	1.35	1.91	2.76	4.44	1.95	1.68	1.28	6.41	2.74
FeO	8.72	10.00	8.72	2.86	8.00	7.20	7.28	10.00	10.08	8.00	6.24	8.32	8.80	9.36	4.61	9.04
MnO	0.18	0.20	0.17	0.17	0.18	0.17	0.17	0.19	0.18	0.18	0.17	0.18	0.17	0.17	0.17	0.18
MgO	8.53	8.87	9.22	8.90	9.52	8.94	7.88	8.60	8.61	8.73	8.81	9.25	8.68	9.08	6.69	7.18
CaO	11.57	10.20	12.19	11.14	11.03	10.86	10.51	10.91	11.14	10.45	11.59	11.51	11.19	11.00	8.82	10.09
Na <sub>2</sub> O	2.26	2.15	2.29	2.65	2.60	2.43	2.63	2.93	2.79	2.69	2.48	2.50	2.55	2.54	3.08	2.93
K <sub>2</sub> O	0.28	0.40	0.11	0.33	0.32	0.39	0.72	0.42	0.43	0.38	0.17	0.28	0.26	0.50	1.79	1.23
P <sub>2</sub> O <sub>5</sub>	0.24	0.42	0.11	0.16	0.26	0.31	0.34	0.22	0.41	0.19	0.10	0.13	0.17	0.23	0.54	0.40
L.O.I.	0.97	1.53	0.89	0.60	0.59	0.44	0.85	0.49	0.86	1.46	0.65	0.93	0.80	0.82	0.61	0.87
TOTAL	99.37	99.91	100.39	100.65	99.86	99.51	99.97	100.69	100.34	99.60	99.53	101.04	98.95	100.02	100.20	101.59
Trace elements in ppm																
Rb	5.6	6.7	2.1	5.9	5.0	7.9	15	6.3	8.1	5.7	2.7	2.3	4.4	8.7	41	27
Sr	213	292	159	273	229	275	305	261	257	241	191	196	242	282	476	460
Y	33	40	22	23	27	28	27	28	33	22	20	21	23	22	26	30
Zr	144	152	45	96	103	123	131	105	156	86	53	69	88	94	198	174
Nb	9.6	14.9	1.8	8.4	10.4	11.7	16.0	9.8	15.6	10.5	3.3	2.6	7.3	13.7	43.6	32.3
Ni	88	165	152	149	138	141	124	125	130	127	147	183	137	140	86	85
Ga	18.5	18.7	16.3	16.3	17.4	18.4	18.3	19.0	20.2	17.5	18.4	16.3	18.7	18.3	17.9	18.5
Cu	54	74	79	64	61	80	60	73	79	85	84	117	79	74	51	63
Zn	98	119	62	75	76	83	95	89	92	72	71	76	75	77	83	95
U	0.4	—	—	1.3	1.0	0.4	—	—	—	—	0.7	—	0.5	—	2.2	1.0
Th	2.0	—	1.3	0.1	1.3	0.1	1.5	0.4	0.9	—	0.2	—	—	1.4	3.3	2.3
Ba	321	2559	454	141	259	210	404	236	249	130	113	192	116	207	653	499
Ce	23	31	17	25	30	37	34	27	34	23	13	15	21	28	51	43
Co	43	52	49	50	47	45	51	48	47	45	43	50	50	50	43	42
La	12	16	6	10	12	17	13	10	15	12	4	9	8	13	29	22
Cr	306	320	278	—	313	301	253	219	232	270	318	278	240	235	129	132
V	275	277	243	—	249	254	268	265	254	247	253	229	254	248	180	231
Sc	38.1	34.1	37.7	—	36.3	37.0	31.5	34.1	34.0	32.1	35.9	34.6	35.6	31.9	23.0	28.4
<sup>87</sup> Sr/ <sup>86</sup> Sr	0.70658	0.70713	0.70591	0.70457	0.70528	0.70502	0.70549	0.70533	0.70541	0.70476	0.70523	0.70462	0.70435	0.70479	0.70390	0.70486
Age (Ma)	7.58	7.20	5.04	4.09	4.06	3.84	1.86	1.55	1.49	1.25	0.91	0.44	0.44	0.36	0.25	*0
Latitude	42.55	42.62	42.14	43.21	43.21	43.14	42.96	42.89	42.79	42.83	42.83	43.22	43.08	42.63	43.03	43.00
Longitude	117.18	117.33	117.31	117.60	117.60	117.39	117.41	117.60	117.60	117.74	117.74	118.34	117.29	117.73	117.43	117.42

Table 2. Continued.

	Samples:													
	JC-4	H86-12	H86-10	H86-62	H86-1	JC-5	JC-3	H86-63	JC-30B	JC-33	H86-64	85-28B	H86-66	H86-2
<b>Major oxides in wt. %</b>														
SiO <sub>2</sub>	47.53	47.73	48.20	47.36	46.99	48.34	48.25	47.66	48.43	48.11	47.18	47.24	48.08	47.35
TiO <sub>2</sub>	2.16	2.21	1.86	2.11	2.16	1.78	1.79	2.11	1.72	1.69	2.11	2.21	2.17	2.17
Al <sub>2</sub> O <sub>3</sub>	15.98	16.31	16.63	16.01	15.97	16.25	15.97	15.98	15.97	16.20	16.02	15.96	16.12	15.90
Fe <sub>2</sub> O <sub>3</sub>	2.31	1.81	1.52	2.41	2.47	1.75	2.21	2.92	2.04	2.25	4.03	4.16	3.85	6.05
FeO	8.55	8.97	8.44	8.34	8.29	7.84	7.60	7.47	7.46	7.22	6.88	6.81	6.62	5.30
MnO	0.17	0.16	0.17	0.17	0.17	0.16	0.16	0.15	0.15	0.16	0.16	0.17	0.15	0.17
MgO	9.29	9.00	8.24	8.95	9.11	8.62	8.53	8.53	9.13	9.00	8.74	8.51	8.83	9.46
CaO	9.93	9.94	10.45	9.40	9.94	9.98	10.26	9.26	9.85	10.23	9.27	9.60	9.68	9.84
Na <sub>2</sub> O	3.08	2.93	3.03	3.21	3.04	2.67	3.01	2.85	3.07	2.80	3.10	3.39	3.26	2.86
K <sub>2</sub> O	0.69	0.72	1.02	0.68	0.69	1.00	1.00	0.71	0.96	0.94	0.71	0.74	0.70	0.69
P <sub>2</sub> O <sub>5</sub>	0.29	0.32	0.39	0.31	0.30	0.41	0.41	0.37	0.43	0.37	0.29	0.32	0.36	0.30
L.O.I.	0.15	0.40	0.57	0.51	0.69	0.80	0.58	1.19	0.31	0.58	1.10	0.51	0.63	0.34
Total	100.13	100.50	100.32	99.46	99.82	99.60	99.77	99.20	99.52	99.55	99.59	99.62	100.45	100.43
<b>Trace elements in ppm</b>														
Rb	12	20	26	12	12	17	17	12	19	16	15	13	15	20
Sr	655	670	484	668	653	486	498	586	528	502	675	671	585	655
Y	23	28	26	25	26	26	25	24	25	25	35	30	25	34
Zr	117	131	180	121	128	162	157	96	126	136	126	127	91	134
Nb	17.9	—	—	—	—	—	—	—	—	—	—	—	—	—
Ni	156	159	118	180	189	118	120	166	155	120	178	158	153	187
Ga	18.1	—	—	—	—	—	—	—	—	—	—	—	—	—
Cu	65	—	—	—	—	—	—	—	—	—	—	—	—	—
Zn	84	—	—	—	—	—	—	—	—	—	—	—	—	—
U	0.7	—	—	—	—	—	—	—	—	—	—	—	—	—
Th	0.4	—	—	—	—	—	—	—	—	—	—	—	—	—
Ba	262	215	230	240	212	251	240	254	238	244	259	252	277	225
Ce	27	23	39	27	27	40	—	29	34	35	27	29	27	26
Co	49	—	—	—	—	—	—	—	—	—	—	—	—	—
La	12	9	18	11	12	18	—	12	17	16	12	12	12	11
Cr	188	202	251	187	204	264	245	208	289	261	194	178	187	200
V	208	209	239	207	223	226	227	207	191	207	209	210	196	226
Sc	27.9	—	—	—	—	—	—	—	—	—	—	—	—	—
<sup>87</sup> Sr/ <sup>86</sup> Sr	0.70382	0.70385	0.70405	0.70384	0.70383	0.70398	0.70398	0.70385	0.70406	0.70401	0.70385	0.70382	0.70384	0.70383
Age (Ma)	*0	*0	*0	*0	*0	*0	*0	*0	*0	*0	*0	*0	*0	*0
Latitude	43.15	43.15	43.15	43.15	43.15	43.15	43.15	43.15	43.16	43.15	43.15	43.15	43.15	43.15
Longitude	117.46	117.50	117.50	117.50	117.50	117.50	117.50	117.50	117.40	117.50	117.50	117.50	117.50	117.50

activity, and some more evolved members representing the earlier pulse of activity.

Figures 5 and 6 illustrate the relationships between selected major and trace elements and MgO. MgO is used here as an indicator of overall degree of basalt differentiation. Given the wide range in ages, vent locations, and  $^{87}\text{Sr}/^{86}\text{Sr}$  ratios of these basalts (Figures 3 and 4), there is no reason to consider trends between age groups to be

indicative of differentiation from a common parental magma. However, major element variations within each age group (Figure 5), such as decreasing  $\text{SiO}_2$  and  $\text{CaO}$  and increasing  $\text{TiO}_2$ ,  $\text{K}_2\text{O}$ , and  $\text{P}_2\text{O}_5$  with decreasing MgO, do suggest that fractional crystallization has played a significant role in Owyhee Plateau basalt evolution, particularly in the two older (Steens Basalt) age groups. In addition, the wide range of  $\text{CaO}$ ,  $\text{Al}_2\text{O}_3$ ,  $\text{TiO}_2$ ,  $\text{K}_2\text{O}$ , and  $\text{P}_2\text{O}_5$

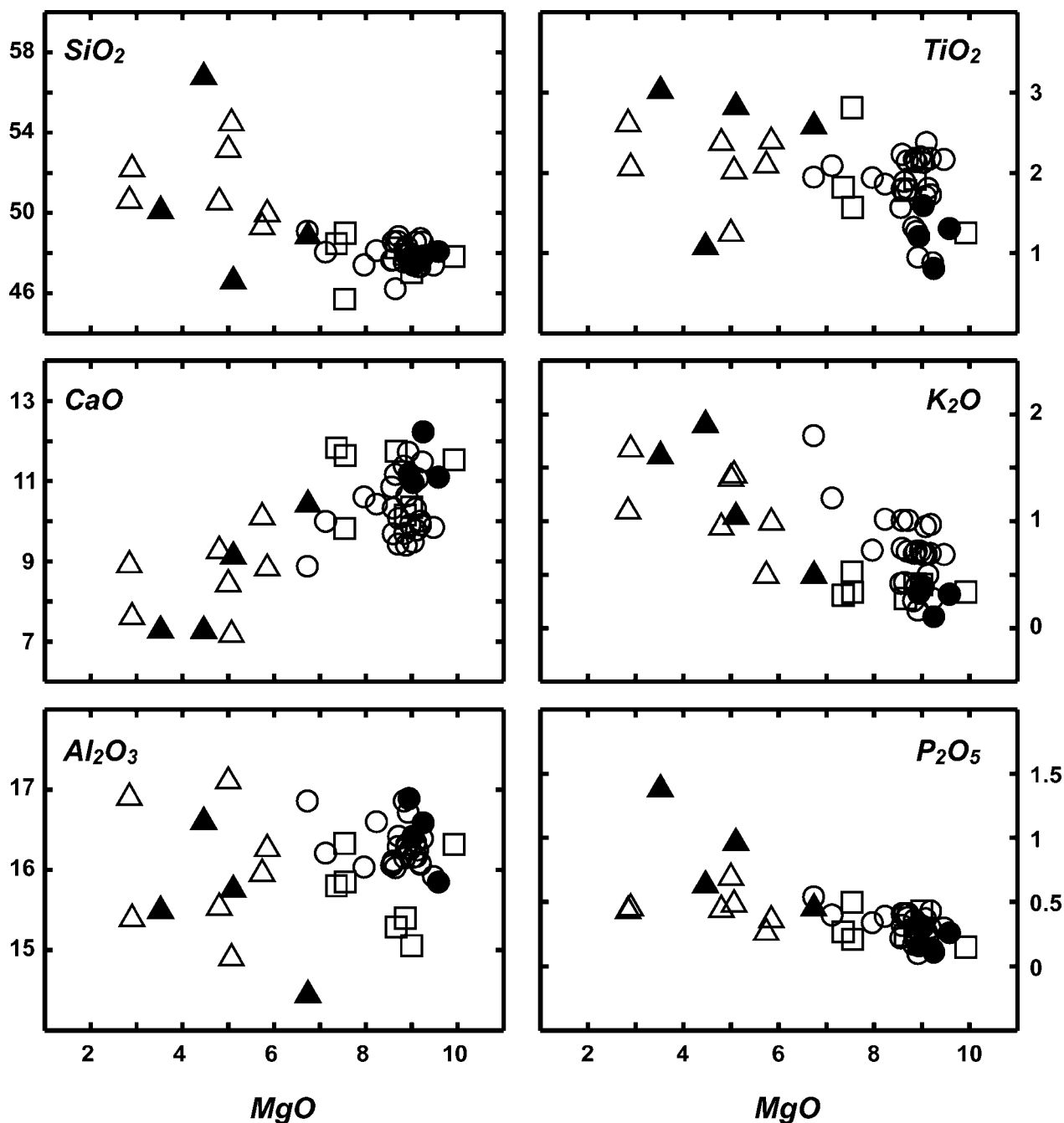


Figure 5. Major element variations with MgO content. Symbols are explained in Figure 4. All oxides reported in weight percent.

contents at the high MgO end of the spectrum suggests that variable depths and degrees of partial melting or the melting of heterogeneous source lithologies, or both, have exerted a primary control on basalt chemical signatures.

The trace element characteristics illustrated in Figure 6 support the above suggestions. For example, the correlated decreases in Ni and MgO within most age groups and decreases in Sc and MgO within the 14-17.5 Ma group suggest olivine fractionation was ubiquitous and hint that

clinopyroxene removal was important during the protracted crystallization experienced by pre-11 Ma basalts. The large ion lithophile (Ba), light rare-earth (La), and high field strength (Zr) element variations also are consistent with variable degrees of crystallization, but the scatter in Ba and Zr above approximately 8 weight percent MgO suggests that multiple geochemical reservoirs probably contributed to the overall geochemical patterns. The most intriguing relationships are displayed in the Sr

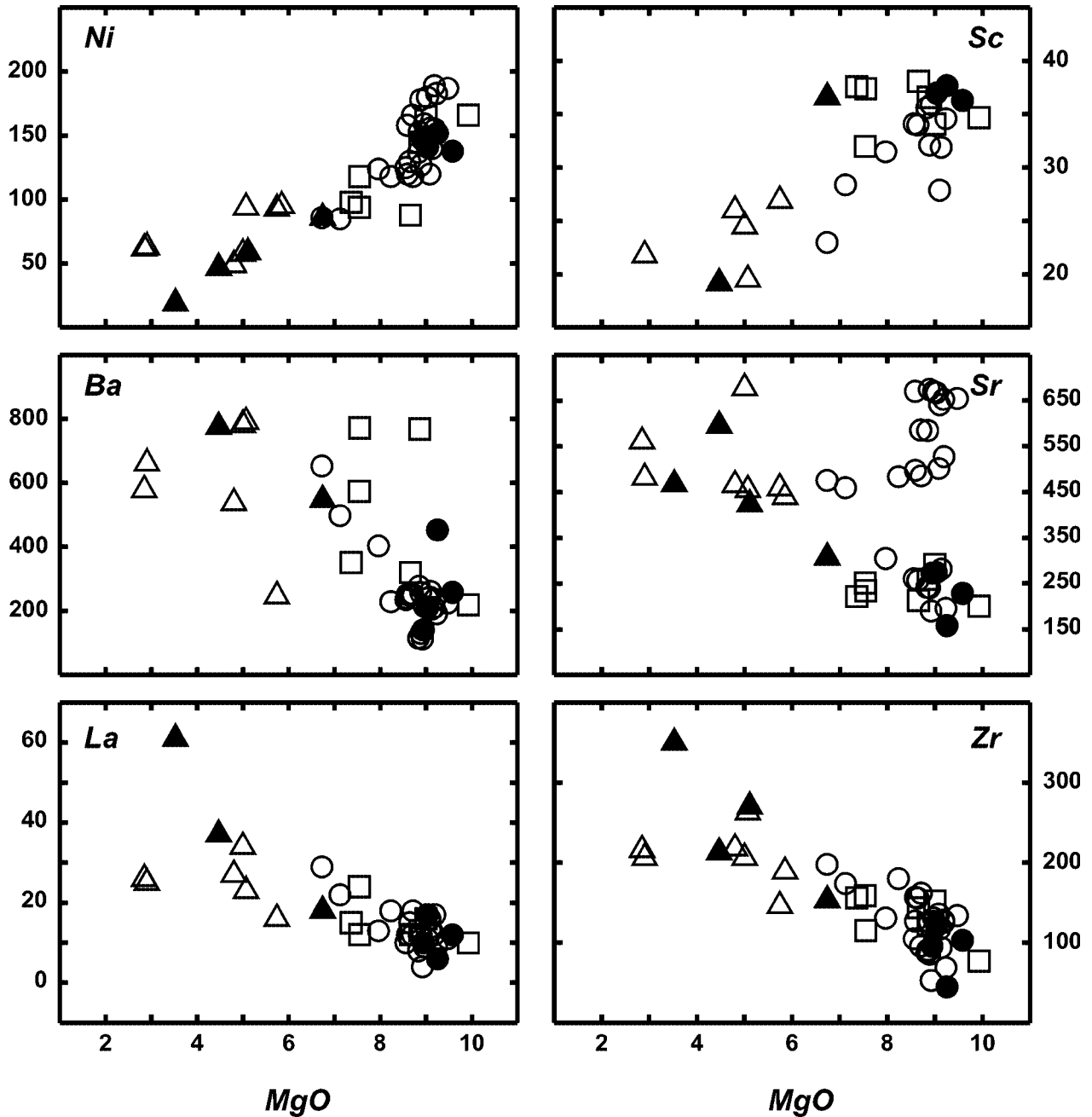


Figure 6. Trace element variations with MgO content. Symbols are explained in Figure 4. All trace elements reported in ppm.

versus MgO plot. The basalt suite is divided into high Sr (greater than 400 ppm) and low Sr (less than 300 ppm) groups. The high Sr samples span the entire observed range of differentiation and include all of the younger than 1 Ma mildly alkaline basalts and most of the older than 11 Ma lavas. These relationships, particularly the occurrence of high (approximately 650 ppm) and low (approximately 200 ppm) Sr content samples at identical high (approximately 9 weight percent) MgO contents, again suggest an important role for partial melting or source composition complexities.

The combined incompatible element characteristics of the least fractionated members of each eruptive age group (i.e., samples with high  $Mg^{2+}/(Mg^{2+}+Fe^{2+})$  (Mg number), high Ni, and low  $SiO_2$ ) are illustrated in the NMORB normalized trace element diagram of Figure 7. These samples have similar overall patterns characterized by strong relative enrichments in Ba and lesser relative enrichments in Nb. The sample with the most MORB-like affinities from La through Y (less than 3 Ma HAOT) has the lowest concentrations of all elements shown, yet still has Sr, K, Rb, and particularly Ba concentrations in excess of NMORB. These characteristics have previously been suggested to indicate a back-arc basin tectonomagmatic setting (Hart and others, 1984; Hart, 1985). Although similar patterns are observed through time, the absolute abundances appear to change as a function of time, as do many incompatible element ratios. These features suggest that similar heterogeneous magma sources and differentiation processes have been involved, but to varying degrees as a function of time, in the evolution of Owyhee Plateau basaltic magmatism.

As shown in Figure 3, basalts from the Owyhee Plateau have a wide range in Sr-isotope values. Close examination of these Sr-isotope characteristics for basalts

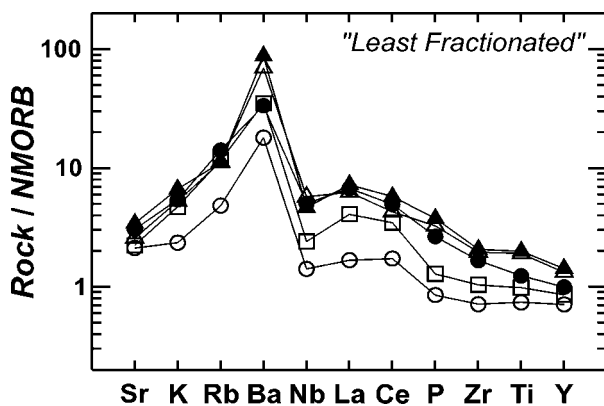


Figure 7. NMORB normalized spider diagram of trace element characteristics of samples representing the least fractionated members of each age group. Symbols are explained in Figure 4.

restricted to the area outlined in Figure 2b reveals an intriguing relationship between the initial  $^{87}Sr/^{86}Sr$  composition and the age of eruption (Figure 8). The most radiogenic Sr is associated with the basalts erupted between 11 and 6 Ma, coincident with the regional change in dominant basalt type erupted (Figure 2a). The systematic decrease in  $^{87}Sr/^{86}Sr$  from this maximum to values less than or equal to 0.704 in both the oldest and youngest basalts implies a decoupling between isotope and bulk chemical characteristics.

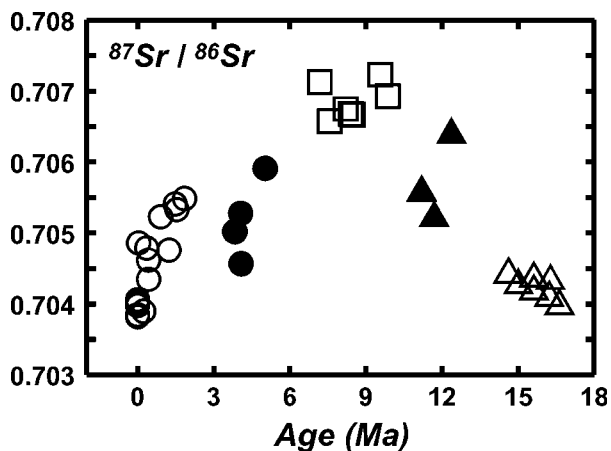


Figure 8. Variations in Sr isotope composition of Owyhee Plateau basalts with age of eruption. Symbols are explained in Figure 4. Samples plotted in this figure include only those thought to be erupted from within the area outlined in Figure 2b, thus not all Oregon Plateau samples plotted in Figure 3 are included. Note that the peak in  $^{87}Sr/^{86}Sr$  around 11 Ma coincides with both the change in dominant basalt type erupted and the onset of Oregon Plateau-wide lithospheric extension.

## DISCUSSION

The data so far presented clearly illustrate that Owyhee Plateau basalt bulk chemical, trace element, and isotopic parameters vary as a function of age. These variations, while systematic, often are decoupled. For example, basalts with Mg number values around 60 span nearly the entire Sr isotopic range. The discussion below focuses on these issues in an attempt to understand the processes leading to the observed features.

Figure 9 illustrates the relationships between the Sr isotopic composition and the Sr concentration and Rb/Sr ratios of the Owyhee Plateau basalts. Samples with Sr contents less than 300 ppm span a range of  $^{87}Sr/^{86}Sr$  from 0.7043 to the highest value measured at 0.7072 (Figure 9a). These samples have Rb/Sr ratios between approximately 0.01 and 0.05 (Figure 9b). In contrast, samples with Sr contents in excess of 400 ppm have Rb/Sr ratios that range from 0.01 to 0.09 and a more limited range in

$^{87}\text{Sr}/^{86}\text{Sr}$  from 0.7038 to 0.7055. In particular, post-1 Ma and pre-14 Ma high Sr concentration samples (with one exception) all have  $^{87}\text{Sr}/^{86}\text{Sr}$  values less than 0.7045 and define within age group trends of nearly constant  $^{87}\text{Sr}/^{86}\text{Sr}$  with increasing Rb/Sr. Similar trends with flat or slightly positive slopes in  $^{87}\text{Sr}/^{86}\text{Sr}$  versus Rb/Sr are observed for all other age groups with the exception of the 14-11 Ma Steens Basalts. Although defined by only three samples in Figure 9, the 14-11 Ma group occupies an intriguing “intermediate” position in terms of combined Sr concentration,  $^{87}\text{Sr}/^{86}\text{Sr}$ , and Rb/Sr characteristics. These characteristics may in part reflect mixing between an end member with high  $^{87}\text{Sr}/^{86}\text{Sr}$  and low Sr and Rb/Sr (11-6 Ma basalts) and an end member with low  $^{87}\text{Sr}/^{86}\text{Sr}$  and high Sr and Rb/Sr (high Sr sample suite).

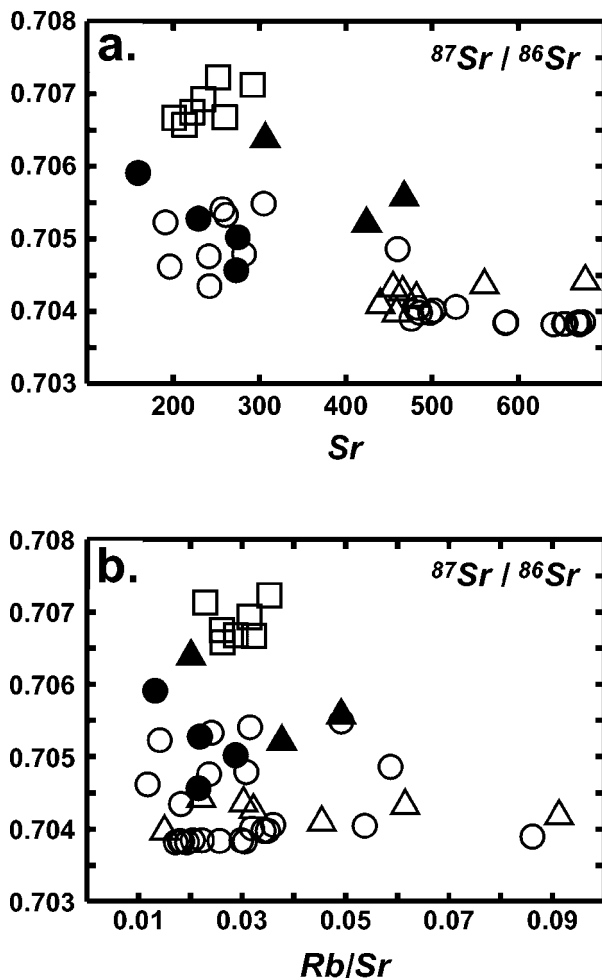


Figure 9. Variations in Sr isotope composition with Sr concentration and Rb/Sr ratio in the context of the eruptive age groups. (a) Relationship between  $^{87}\text{Sr}/^{86}\text{Sr}$  and Sr concentration. (b) Relationship between  $^{87}\text{Sr}/^{86}\text{Sr}$  and Rb/Sr ratio. Symbols are explained in Figure 4.

The above relationships do not rule out a role for felsic upper crustal contamination that in the Owyhee Plateau area could involve heterogeneous lithologies with  $^{87}\text{Sr}/^{86}\text{Sr}$  of 0.705 to greater than 0.710 (Leeman and others, 1992 and references therein). For example, contamination of a low Sr concentration basaltic magma by felsic material at the radiogenic end of this range certainly could contribute to the high  $^{87}\text{Sr}/^{86}\text{Sr}$  of the 11-6 Ma group. Such a contaminant would likely have an elevated Rb/Sr ratio; thus the low Rb/Sr ratios of the 11-6 Ma basalts are at odds with significant felsic crustal addition. This interpretation is extended to the remainder of the Owyhee Plateau basalt suite considering the observed within-group  $^{87}\text{Sr}/^{86}\text{Sr}$ , Rb/Sr, and Sr concentration relationships. Therefore, we interpret the relationships displayed in Figure 9 to indicate that felsic crustal contamination was not a dominant contributor to the overall geochemical characteristics observed, that distinct mantle source reservoirs were involved in Owyhee Plateau magma generation, and that magmas erupted just before the regional change in basalt geochemistry at approximately 11 Ma may preserve evidence for a combination of pre- and post-11 Ma source and process inputs.

Additional combined chemical and Sr isotope characteristics of basalts from the Owyhee Plateau are illustrated in Figure 10 in the context of the eruptive age groups. The decoupling of isotope and chemical characteristics is further highlighted by examining variations in differentiation indices such as Mg number (Figure 10a) and trace element ratios such as K/P and Zr/Nb (Figure 10b, 10c) relative to the age of eruption and Sr isotope compositions.

The plot of Mg number versus age (Figure 10a) again illustrates the regional change from strongly fractionated basalts and basaltic andesites before about 11 Ma to relatively unfractionated basalts after about 11 Ma. The same Sr isotope composition, however, can occur over a wide range of Mg number values. This implies that upper crustal assimilation accompanying crystal fractionation exerted little influence on the observed Sr isotope compositions. Thus, the first-order variations in isotopic composition are likely due to variations in relative contributions from different mantle sources through the course of Owyhee Plateau development.

The K/P ratio (Figure 10b) has been used to monitor contamination of low K/P mafic magmas by high K/P upper crustal materials (Carlson and Hart, 1987). In the Owyhee Plateau basalt suite K/P shows the least crustlike signatures at the most radiogenic Sr isotope values, and vice versa. Thus, if crustal contamination is occurring, either it is not the dominant factor controlling the chemical characteristics of these basalts, or it is taking place at

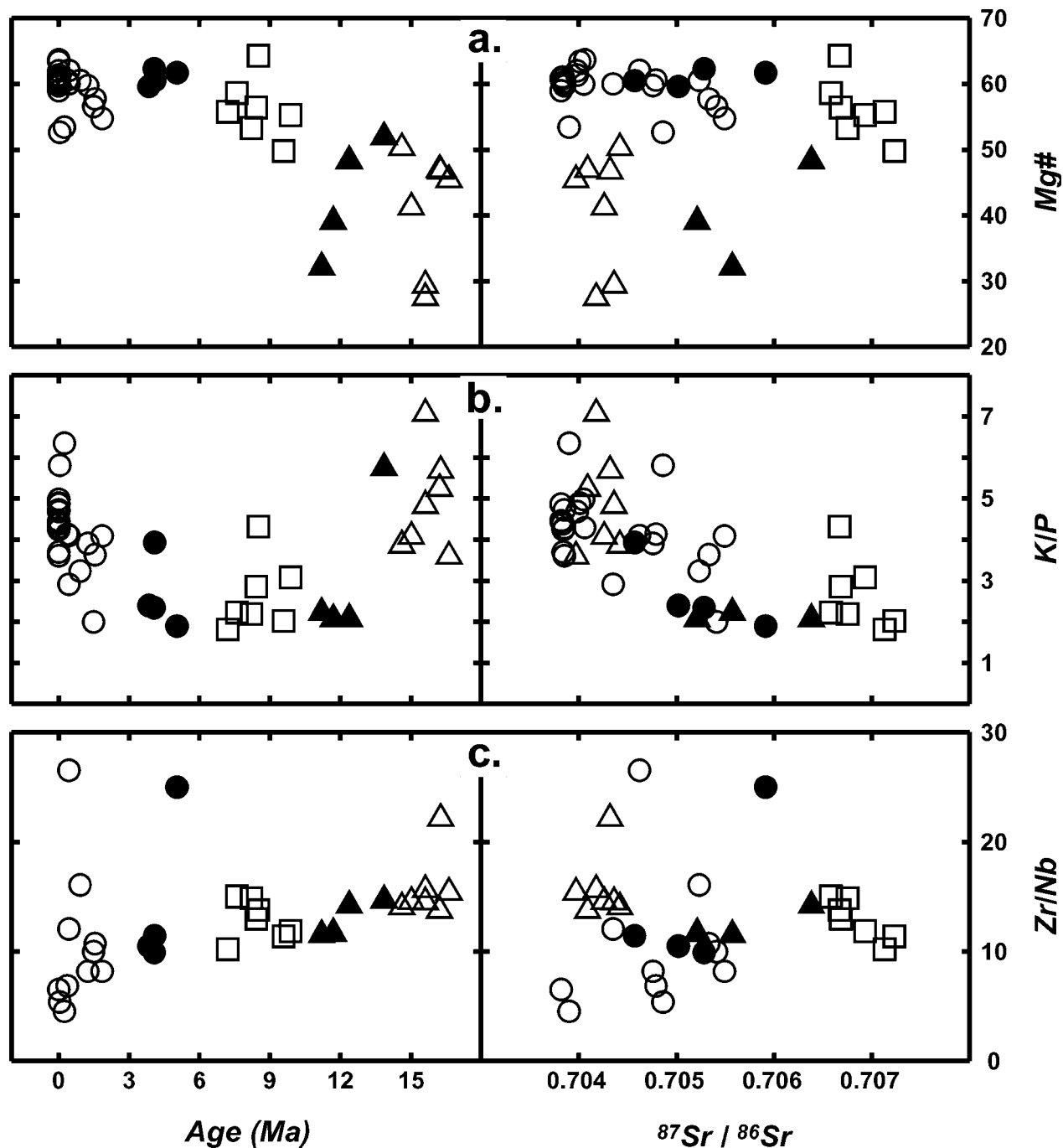


Figure 10. Variations in Mg number, K/P, and Zr/Nb in Owyhee Plateau basalts with age and  $^{87}\text{Sr}/^{86}\text{Sr}$ . Symbols are explained in Figure 4.

depth where the crust is likely to be more “basaltic” in composition. The relationships may be best explained by changes in the relative contributions of various source reservoirs. For example, the high  $^{87}\text{Sr}/^{86}\text{Sr}$  values seen in the basalts erupted during the change in basalt geochemistry (approximately 11 Ma) may represent melts derived dominantly from the subcontinental lithospheric mantle

(SCLM) that subsequently interacted little with upper crustal rocks or melts. The older and younger basalts may have a more complex history involving a larger contribution from less radiogenic sublithospheric mantle sources plus relatively greater, but still minimal amounts of local crustal contamination. If this is the case, it is significant that the peak in  $^{87}\text{Sr}/^{86}\text{Sr}$  values and the change

in basalt chemistry approximately coincide with the onset of Oregon Plateau-wide lithospheric extension (Hart and Carlson, 1987; Hooper, 1990; Draper, 1991). Such extension would significantly thin the lithosphere, allowing decompression melting of the SCLM (McKenzie and Bickle, 1988; Gallagher and Hawkesworth, 1992). It would also significantly reduce the thickness of crust that the magmas would have to traverse before eruption, resulting in less differentiated basalt chemistries.

In contrast to K/P, Zr/Nb (Figure 10c) appears only to decrease slightly with decreasing age throughout the full age spectrum. Zr and Nb should not be fractionated from each other during typical melting or crystallization processes in relatively anhydrous basaltic systems. While this trend is also apparently decoupled from the trend in  $^{87}\text{Sr}/^{86}\text{Sr}$  values, the implications of this relationship are not as clear. Only a few outliers in the data set, however, approach normal MORB values ( $\text{Zr}/\text{Nb} = 30$ ); most samples fall in between values for continental crust and ocean island basalts (Weaver, 1991). These characteristics may lend support to the presence of subduction-modified sublithospheric upper mantle beneath the Owyhee Plateau (Carlson and Hart, 1987; Hart and others, 1997).

The aforementioned relationships suggest that the temporal development of rifting and extension in this narrowly defined region of transitional lithosphere is exerting a strong control on (1) basalt source parameters, in particular the reservoirs involved in the genesis of these magmas, and their relative contributions at various stages during the past 17.5 Ma; and (2) the subsequent magmatic differentiation histories of these basalts.

In light of these observations, the following preliminary model is offered and is keyed to the Sr isotope versus age plot of Figure 11.

*Stage 1.* The initial, 17.5-14 Ma, large volume flood basalts are generated from hot, upwelling sublithospheric mantle. Although these magmas may be contaminated by small amounts of melt from the SCLM and by crustal lithologies, they retain their less radiogenic Sr isotopic signature because the volume of sublithospheric mantle-derived melt is so great. In addition, these basalts have Sr concentrations in excess of 400 ppm, thus further minimizing the effects of crustal contamination accompanying upper level differentiation on the Sr isotopic composition. Significant residence time in crustal magma chambers is suggested by the evolved bulk compositions characteristic of this time interval and is consistent with the presence of thick crust at the onset of rifting.

*Stage 2.* The waning stages of the Steens Mountain Basalt eruptions (14-11 Ma) reflect smaller volumes of melt being generated from the sublithospheric mantle. These melts interact with melts of the SCLM as before. However, because the volume of sublithospheric mantle-

derived melt is now much less, melts derived from the SCLM exert a stronger control on the Sr isotopic composition and trace element characteristics of the resulting magmas (Figures 9, 10a, and 10c)

*Stage 3.* The onset of Oregon Plateau-wide lithospheric extension at about 11 Ma allows decompression melting of the SCLM, particularly easily melted mafic constituents (Harry and Leeman, 1995). Basalts erupted during the 11-6 Ma interval reflect the higher  $^{87}\text{Sr}/^{86}\text{Sr}$  values of the SCLM materials as melts derived therefrom dominated over sublithospheric melts. Crustal residence time and input are less significant during this interval due to the active extension of already thinned crust. While some degree of crustal contamination cannot be ruled out, its influence on basalt chemistry is more cryptic. This may reflect the involvement of more mafic crustal lithologies present as a result of the previous pulses of flood basalt activity.

*Stage 4.* With much of the easily melted portion of the SCLM removed, small volume magmas are produced that represent varying degrees of mixing between sublithospheric and SCLM melts, with the contribution from the SCLM lowest in the young, mildly alkaline basalts. Thus, basalts erupted during short intervals between 6 Ma and the present have more widely varying geochemical signatures.

Further testing and refinement of this model await further detailed modeling of possible basalt source melting scenarios and melt regime physical parameters as well as Nd, Pb, and Os isotopic work on samples spanning the ranges shown in Figures 9-11. In addition, further field and analytical work is in progress south of the area shown in Figure 1b in a region where numerous basalt vent localities have been identified.

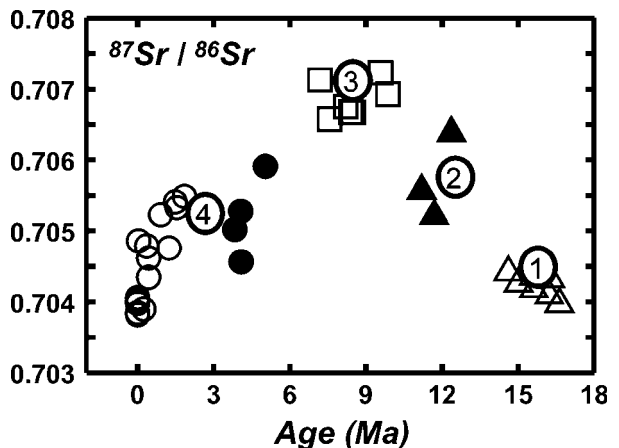


Figure 11. Preliminary model for the development of observed Sr isotope and geochemical characteristics of Owyhee Plateau basalts. Symbols are explained in Figure 4.

## CONCLUSIONS

The observed geochemical and isotopic diversity in Owyhee Plateau basalts apparently cannot be attributed solely to lateral lithospheric heterogeneities or to crustal contamination accompanying upper-level differentiation. Rather, this diversity appears to be a function of the age of eruption. Furthermore, the first-order processes responsible for the generation and evolution of these magmas are apparently controlled by temporal variations not only in magmatic volume and lithospheric structure, but also in relative contributions from lithospheric and sublithospheric source reservoirs. The results of this study emphasize the importance of time as a variable in evaluating the evolution of magmas, magmatic processes, and magma source regions in complex continental igneous provinces.

## ACKNOWLEDGMENTS

The authors gratefully acknowledge financial support from the Geological Society of America (Lipman Research Award, 5929-96; Shoemaker), the National Science Foundation (EAR-9204780; Hart), the Miami University Graduate School Dissertation Research Support Fund (Shoemaker), the Miami University Committee on Faculty Research (Hart), and the Miami University Geology Department. We would like to thank Stan Mertzman of Franklin and Marshall College for making his XRF facility available, and John Morton of Miami University for his assistance with the Sr isotope and DCP major and trace element analyses. Our gratitude is also extended to Matt Heizler of the New Mexico Geochronological Research Laboratory for performing the  $^{40}\text{Ar}/^{39}\text{Ar}$  analyses. Reviews by Roger Stewart, Craig White, and Scott Hughes helped to clarify the content and improve the readability of this contribution.

## REFERENCES

- Bohannon, R.G., and T. Parsons, 1995, Tectonic implications of post-30 Ma Pacific and North American relative plate motions: *Geological Society of America Bulletin*, v. 107, p. 937-959.
- Boyd, F.R., and S.A. Mertzman, 1987, Composition and structure of the Kaapvaal lithosphere, southern Africa, in B.O. Mysen, ed., *Magmatic Processes—Physicochemical Principles: The Geochemical Society Special Publication 1*, p. 13-24.
- Camp, V.E., 1995, Mid-Miocene propagation of the Yellowstone mantle plume head beneath the Columbia River basalt source region: *Geology*, v. 23, p. 435-438.
- Carlson, R.W., 1984, Isotopic constraints on Columbia River flood basalt genesis and the nature of the subcontinental mantle: *Geochimica et Cosmochimica Acta*, v. 48, p. 2357-2372.
- Carlson, R.W., and W.K. Hart, 1987, Crustal genesis on the Oregon Plateau: *Journal of Geophysical Research*, v. 92, p. 6191-6206.
- , 1988, Flood basalt volcanism in the northwestern United States, in J.D. Macdougall, ed., *Continental Flood Basalts: Kluwer Academic Publishers*, p. 35-61.
- Carlson, R.W., G.W. Lugmair, and J.D. Macdougall, 1981, Columbia River volcanism: The question of mantle heterogeneity or crustal contamination: *Geochimica et Cosmochimica Acta*, v. 45, p. 2483-2499.
- Christiansen, R.L., and E.H. McKee, 1978, Late Cenozoic volcanic and tectonic evolution of the Great Basin and Columbia intermontane regions, in R.B. Smith and G.P. Eaton, eds., *Cenozoic Tectonics and Regional Geophysics of the Western Cordillera: Geological Society of America Memoir 152*, p. 283-311.
- Draper, D.S., 1991, Late Cenozoic bimodal magmatism in the northern Basin and Range Province of southeastern Oregon: *Journal of Volcanology and Geothermal Research*, v. 47, p. 299-328.
- Elison, M.W., R.C. Speed, and R.W. Kistler, 1990, Geologic and isotopic constraints on the crustal structure of the northern Great Basin: *Geological Society of America Bulletin*, v. 102, p. 1077-1092.
- Ferns, M.L., 1997, Field trip guide to the eastern margin of the Oregon-Idaho graben and the middle Miocene calderas of the Lake Owyhee volcanic field: *Oregon Geology*, v. 59, p. 9-20.
- Gallagher, Kerry, and Chris Hawkesworth, 1992, Dehydration melting and the generation of continental flood basalts: *Nature*, v. 358, p. 57-59.
- Geist, Dennis, and Mark Richards, 1993, Origin of the Columbia Plateau and Snake River Plain: Deflection of the Yellowstone plume: *Geology*, v. 21, p. 789-792.
- Harry, D.L., and W.P. Leeman, 1995, Partial melting of melt metasomatized subcontinental mantle and the magma source potential of the lower lithosphere: *Journal of Geophysical Research*, v. 100, p. 10,255-10,269.
- Hart, W.K., 1985, Chemical and isotopic evidence for mixing between depleted and enriched mantle, northwestern U.S.A.: *Geochimica et Cosmochimica Acta*, v. 49, p. 131-144.
- , 1996, Petrogenesis of Quaternary Oregon Plateau alkaline basalts: *Geological Society of America Abstracts with Programs*, v. 28, p. 73.
- , 1997, Plume-asthenosphere-lithosphere interactions through time: A comparison of Ethiopian and northwestern USA basalts: *Geological Society of America Abstracts with Programs*, v. 29, p. 298.
- Hart, W.K., J.L. Aronson, and S.A. Mertzman, 1984, Areal distribution and age of low-K, high-alumina olivine tholeiite magmatism in the northwestern Great Basin: *Geological Society of America Bulletin*, v. 95, p. 186-195.
- Hart, W.K., and R.W. Carlson, 1983, K-Ar ages of late Cenozoic basalts from southwestern Oregon, southwestern Idaho, and northern Nevada: *Isochron/West*, v. 38, p. 23-26.
- , 1985, Distribution and geochronology of Steens Mountain-type basalts from the northwestern Great Basin: *Isochron/West*, v. 43, p. 5-10.
- , 1987, Tectonic controls on magma genesis and evolution in the northwestern United States: *Journal of Volcanology and Geothermal Research*, v. 32, p. 119-135.
- , 1992, The development of the Oregon Plateau: Perspectives from Neogene mafic to intermediate volcanism: *Geological Society of America Abstracts with Programs*, v. 24, p. 32.
- Hart, W.K., R.W. Carlson, and S.A. Moshier, 1989, Petrogenesis of the Pueblo Mountains basalt, southeastern Oregon and northern Nevada, in S.P. Reidel and P.R. Hooper, eds., *Volcanism and Tectonism in the Columbia River Flood Basalt Province: Geological Society of America Special Paper 239*, p. 367-378.

- Hart, W.K., R.W. Carlson, and S.B. Shirey, 1997, Radiogenic Os in primitive basalts from the northwestern U.S.A.: Implications for petrogenesis: *Earth and Planetary Science Letters*, v. 150, p. 103-116.
- Hart, W.K., and S.A. Mertzman, 1982, K-Ar ages of basalts from southcentral and southeastern Oregon: *Isochron/West*, v. 33, p. 23-26.
- , 1983, Late Cenozoic volcanic stratigraphy of the Jordan Valley area, southeastern Oregon: *Oregon Geology*, v. 45, p. 15-19.
- Hooper, P.R., 1990, The timing of crustal extension and the eruption of continental flood basalts: *Nature*, v. 345, p. 246-249.
- Hooper, P.R., and C.J. Hawkesworth, 1993, Isotopic and geochemical constraints on the origin and evolution of the Columbia River Basalt: *Journal of Petrology*, v. 34, p. 1203-1246.
- Lambert, R. St.J., V.E. Chamberlain, and J.G. Holland, 1995, Ferro-andesites in the Grande Ronde Basalt: Their composition and significance in studies of the origin of the Columbia River Basalt Group: *Canadian Journal of Earth Sciences*, v. 32, p. 424-436.
- Le Bas, M.J., R.W. Le Maitre, A. Streckeisen, and B. Zanettin, 1986, A chemical classification of volcanic rocks based on the total alkali-silica diagram: *Journal of Petrology*, v. 27, p. 745-750.
- Leeman, W.P., 1982, Tectonic and magmatic significance of strontium isotopic variations in Cenozoic volcanic rocks from the western United States: *Geological Society of America Bulletin*, v. 93, p. 487-503.
- Leeman, W.P., and W.I. Manton, 1971, Strontium isotopic composition of basaltic lavas from the Snake River Plain, southern Idaho: *Earth and Planetary Science Letters*, v. 11, p. 420-434.
- Leeman, W.P., J.S. Oldow, and W.K. Hart, 1992, Lithosphere-scale thrusting in the western U.S. Cordillera as constrained by Sr and Nd isotopic transitions in Neogene volcanic rocks: *Geology*, v. 20, p. 63-66.
- Le Maitre, R.W., 1976, Some problems of the projection of chemical data into mineralogical classifications: *Contributions to Mineralogy and Petrology*, v. 56, p. 181-189.
- Mark, R.K., H.R. Bowman, F. Asaro, E.H. McKee, and R.R. Coats, 1975, A high  $^{87}\text{Sr}/^{86}\text{Sr}$  mantle source for low alkali tholeiite, northern Great Basin: *Geochimica et Cosmochimica Acta*, v. 39, p. 1671-1678.
- McKenzie, D., and M.J. Bickle, 1988, The volume and composition of melt generated by extension of the lithosphere: *Journal of Petrology*, v. 29, p. 625-679.
- Noble, D.C., C.E. Hedge, E.H. McKee, and M.K. Korrinda, 1973, Reconnaissance study of the strontium isotope composition of Cenozoic volcanic rocks in the northwestern Great Basin: *Geological Society of America Bulletin*, v. 84, p. 1393-1406.
- Pierce, K.L., and L.A. Morgan, 1992, The track of the Yellowstone hot spot: Volcanism, faulting, and uplift, in P.K. Link, M.A. Kuntz, and L.B. Platt, eds., *Regional Geology of Eastern Idaho and Western Wyoming*: Geological Society of America Memoir 179, p. 1-53.
- Russell, J.K., G.T. Nixon, and T.H. Pearce, 1988, Petrographic constraints on modeling the crystallization of basalt magma, Cow Lakes, southeast Oregon: *Canadian Journal of Earth Sciences*, v. 25, p. 486-494.
- Sterner, Ray, 1997, Shaded relief map of Oregon: Johns Hopkins University Applied Physics Laboratory, <http://fermi.jhuapl.edu/states>.
- Weaver, B.L., 1991, Trace element evidence for the origin of ocean-island basalts: *Geology*, v. 19, p. 123-126.
- Wright, J.E., and J.L. Wooden, 1991, New Sr, Nd, and Pb isotopic data from plutons in the northern Great Basin, USA: Implications for crustal structure and granite petrogenesis in the hinterland of the Sevier thrust belt: *Geology*, v. 19, p. 457-460.
- Zoback, M.L., E.H. McKee, R.J. Blakely, and G.A. Thompson, 1994, The northern Nevada rift: Regional tectono-magmatic relations and middle Miocene stress direction: *Geological Society of America Bulletin*, v. 106, p. 371-382.